

# Preliminary Results on the Design of a Tool for Inserting of Transverse Intrafascicular Multichannel Electrodes (TIME) into the peripheral nervous system

A. Ghionzoli, V. Genovese, S. Bossi, C. Stefanini, S. Micera, *IEEE Senior Member*

**Abstract**— Transverse intrafascicular multichannel electrodes (TIMEs) are polyimide-based microelectrodes, which are potentially very interesting to restore sensorimotor functions in disabled people. By means of microstimulation of the nerve stump of an amputee, it can be possible to manipulate the phantom limb sensation, to provide sensory feedback to upper limb amputees, and to investigate methods of treatment of phantom limb pain. The current insertion procedure of TIMEs is completely done by hand. This makes the task difficult. This paper presents the preliminary results related to the development of a robotic tool to increase the accuracy in electrode placement and reduced size of the working area. The possibility to manage insertion parameters such as force, velocity, and positioning, could decrease the risk of damaging the nervous tissue, improving the coordination, and making placements repeatable. With the aim of solving the issues above, we developed a first prototype of a 4DoF multi-axis device. Additional strategies concerning system components and control are discussed. We performed characterization of implantation mechanics to derive mechanical design specifications for the robotic device. Force characterization of the pig peripheral nerve during penetration of the needle at three velocities (1, 30, 40mm/sec) was executed. Results shown inverse relationship between maximal force and velocities values. The force values extracted varied between 0.081 – 0.174 N.

## I. INTRODUCTION

The development and implantation of selective invasive interfaces with the peripheral nervous system is an interesting research area for the possible improvements in quality of life which can be due to the use of these technologies. Transverse intrafascicular multichannel electrodes (TIMEs) have shown to be promising interfaces for the control of neuroprostheses and neurocontrolled artificial limbs.

The insertion procedure of TIME electrodes into the peripheral nerves is currently completely done manually by the surgeon [1]. The electrode is designed to be implanted into the nerve transversally, allowing the access to different

subgroups of nerve fibers. Using forceps, the surgeon steer the needle-electrode structure through the nerve, and monitor the positioning of the electrode by a microscope. The coordinated action of both hands of the surgeon is needed, one handling the nerve, to facilitate the entrance of the needle, and the other driving the needle. Referring to surgical application in small spaces, the technical difficulties are mainly related to hand tremor, fatigue [2], [3], and in particular difficulty to placing electrodes with repeatability, and reduced accuracy.

An incorrect procedure may result in lack of repeatability, reduced accuracy, increased implantation time and nerve damage.

With the aim to overcome these issues, we introduced in this paper a new robotic tool able to place TIME electrodes into peripheral nervous tissue. It is well known that the mechatronics is able to improve the efficacy of surgical procedures when precision, dexterity and small dimensions are on the edge of human limits. This area is called Minimal Invasive Surgery (MIS). One of the most difficult tasks required during MIS is to reach the optimal surgical target while controlling force, position and velocity parameters of mechatronic devices [4]. The same requirements are necessary during the insertion of neural interfaces through the peripheral nerve [5]. Zhang et al. developed a two DoF robot able to control the insertion depth and the steering of the electrode array in the cochlea. The work of Taylor et al. is related to a force controlled steady-hand manipulator for retinal microsurgery. Fee et al. described a miniaturized microdrive for independently positioning three electrodes in the brain.

Previous works showd MIS applications in neuroprosthetics for cochlear implant surgery [6], retinal surgery [4], electrode positioning in the brain [7].

Starting from these considerations, in this paper we present a multiaxis mechatronic device controllable by the surgeon, while meeting position accuracy and safety surgical requirements for optimal insertion placement of steerable electrode array. The prototype introduced here concerns the first step on the evolution of a tool conceived to steer TIME electrodes within the sciatic tibial nerve of the rat (approximately 2 mm of diameter).

Because of the small size of the structures involved and the limited access to the surgical site, this new technological approach is motivated by overcoming these issues, by reducing strain in the nervous tissue within a physiological

This work was supported by the EU within the TIME Project (Transverse Intrafascicular Multichannel Electrode system, ICT-2007.3.6 Nano/Micro priority, project number 224012). Website: [www.project-time.eu/](http://www.project-time.eu/).

A. Ghionzoli, V. Genovese, S. Bossi, C. Stefanini, S. Micera are with the BioRobotics Institute, Scuola Superiore Sant'Anna, Pisa, Italy (Corresponding author. e-mail: [a.ghionzoli@sssup.it](mailto:a.ghionzoli@sssup.it)).

S.Micera is with the Automatic Control Laboratory, Swiss Federal Institute of Technology, Zurich, Switzerland.

safety range [8], by putting down the number of failed insertions, enhancing the optimal electrode placement and repeatability in placement. The integration of a force sensor during the electrode penetration may indicate the crossing of the nerve layers [9], and the possibility of insert the electrode within a safe range of forces.

## II. IMPLANT MECHANIC CHARACTERIZATION

### A. TIME Implantation Procedure

The procedure for implanting TIME electrodes is subdivided into several steps, as described by Boretius et al. [1]. Briefly, the electrode is connected to 10-0 suture straight needle (EH 7900 Ethicon stc-6), by means of a loop of kevlar filament to create a linked structure (fig. 2). During implantation procedure the needle crosses transversely the nerve and it is used to push the electrode inside the peripheral nerve. After placing the electrode inside the nerve, the cable is cut and a suture is made to secure the electrode.

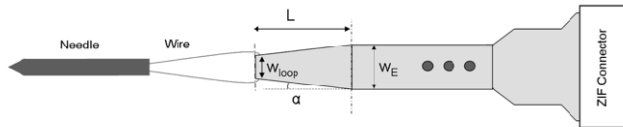


Fig. 1. Schematic of the system needle-wire-NI for NI insertion into peripheral nerves.  $W_{loop}$  is the width of the section at the beginning of the interface,  $W_E$  is the width of the constant section in which active sites are positioned. The electrode samples had a symmetric structure and were composed of a first share with a trapezoidal shape (variable width,  $\alpha$ ) and  $L$  length.

### B. Characterization of implantation forces

To get information on forces involved during needle penetration in peripheral nerve, we conducted *ex-vivo* experiments in pig nerves. The aim of the investigation was to evaluate the forces involved during the piercing of the nerve in a wide range of velocities, and to suggest control strategies minimizing implantation forces on the nerve. We hypothesized that an increase of penetration velocity is associated with a decrease of force [10].

Using the setup illustrated in fig. 2 is used for the characterization of the forces involved during needle penetration in pig peripheral nervous tissue. The test device consisted of a nerve sample locked up in a hold position, a DC linear motor at which is connected a load cell, and a needle (125  $\mu\text{m}$  of diameter) linked in turn to the load cell. A computer connected to the motor controller did the advancement commands. Insertion experiments were performed in median and ulnar nerve specimen of pig (3–4 mm in width and 2–3 mm in thickness). During each insertion the slide moves from  $X = 0$  mm to  $X = 19$  mm with a trapezoidal velocity profile.

The needle insertion force was recorded in a range of velocity between 1 and 50 mm/sec. For each velocity one penetration was done. Force signal coming from the load cell are acquired by a 16-Bit DAQ working at the sample frequency  $F_s = 1\text{K Hz}$ .

The force range is  $\pm 35\text{N}$  while the effective resolution is  $1/160\text{ N}$ .

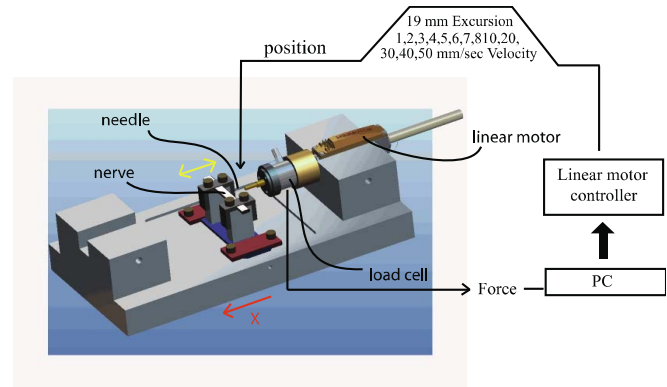


Fig. 2. Experimental Setup. The CAD model illustrate the system used for the characterization of piercing forces in porcine peripheral nerves. The test needle (EH 7900 Ethicon stc-6) is fixed to the load cell (ATI nano 17 SI-25-0.25), which in turn is connected to a linear slide DC Motor (Faulhaber LM1247-040-01). The position of the motor rod is controlled by means of a motion controller (Faulhaber MCLM 3003S). The start and stop positions are driven by a PC. The home made setup allows the measurement of force, speed and position of the needle during the penetration within nerve sample. The nerve is fixed between two clamps. To simulate the implantation procedure we setted the distance between the two clamps at 7 mm.

Figure 3 shows typical force curves of needle insertion at three velocities (1 mm/s, 30 mm/s, and 40 mm/s). The force curves are characterized by significantly different force peaks (about 0.174 N at 1 mm/s, 0.116 at 30 mm/s, and 0.081 N at 40 mm/s) and by an increased regularity of the curves as the the speed increases.

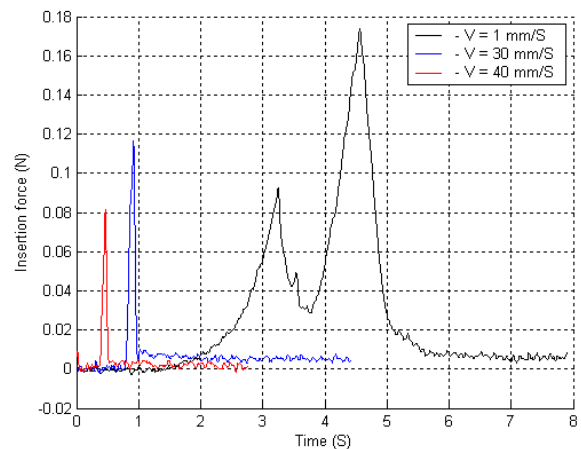


Fig. 3. Typical force curves during experiments of needle insertion in pig peripheral nerve.

In order to evaluate the effect of different types of TIME probes, in terms of force range, during the crossing of peripheral nerves, additional experiments of TIME probe insertion was performed. We recorded the forces due to the

interaction between the tissue and three electrodes shapes (*small, large a, large b*) in a range of low velocities (0.08, 0.8, 1.6 mm/sec). Geometrical differences among electrodes are summarized in table 1.

TABLE I  
GEOMETRICAL PARAMETERS OF TIME ELECTRODES

Electrode Type	$W_{loop}$ ( $\mu\text{m}$ )	$W_E$ ( $\mu\text{m}$ )	L (mm)	$\alpha$ (degree)	Number Of Channels
Large a	100	180	7	0,33	5
Large b	100	260	7	0,66	3
Small	100	280	2	2,57	5

Figure 4 shows typical force curves obtained with three different electrodes at the same velocity (0.8 mm/sec) during the crossing of the nerve. Concerning the maximal force values related to the exit of the main section ( $W_e$ ) from the nerve, we noted significant differences in force peaks (about 0.011 N for *Small* electrode; 0.004 N for *Large a* and about 0.008 N for *Large b*).

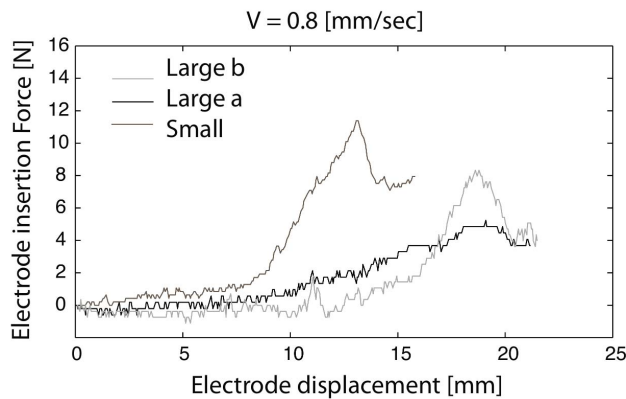


Fig. 4. Electrode insertion curves obtained with *Large a, Large b, Small* electrodes obtained at the same velocity (0.8 mm/sec).

Pertaining to insertions trials at the velocity of 1.6 mm/sec, the peak of force corresponding to the  $W_e$  section (*Large b*) is about 0.015 N, while considering the velocity of 0.08 mm/sec, the maximal force corresponding to  $W_e$  section is about 0.05 N.

## II. MECHANICAL SYSTEM CONCEPT AND SPECIFICATION

The design of our first prototype started with the evaluation of the necessary degrees of freedom used by the surgeon to accomplish the task, and the selection of mechanical parameters such as range of motion, precision, and maximal velocity.

### A. Degrees of Freedom

In this section we analyzed the necessary DoF to perform TIME insertion; we separated the task in main stages in order to assign at each device mechanical component the corresponding function. Starting from the observation of surgical procedure (figure 5), we can detect three main phases:

- A. approach phase. During this phase the surgeon move the needle tip close at the nerve insertion point choosing the insertion angle  $\alpha$  ;
- I. insertion phase. The needle is inserted transversely up the nerve to pass completely through with the departure angle  $\beta$ .
- P. electrode placement phase. The surgeon takes out the needle from the nerve and then dragging the electrode in the right position.

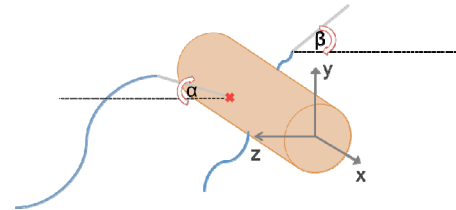


Fig. 5. Setup of surgical procedure. In this sketch is illustrated the approach – insertion angle ( $\alpha$ ) and the evacuation angle ( $\beta$ ) used to drive the needle electrode framework into the peripheral nerve. During the approach phase, the end effector can rotate in the range of  $\alpha = \pm 90^\circ$ , the same range of rotation is allowed to insert the needle, during the I phase. Finally the placement of the electrode will result in a combination of  $\alpha$  rotations. The second end effector, that is devoted to the placement of the electrode, can rotate in a range of  $\beta = \pm 90^\circ$ .

Each phase requires an adequate number of degrees of freedom: in the approach phase the surgeon requires at least 4 DoF ( $x, y, z, M_x$ ), in the insertion phase the DoF are 3 ( $M_x, y, z$ ), and during electrode placement phase 3 DoF ( $M_x, y, z$ ).

Taking into account the size of the rat, the size of surgical area, the location of the nerve, the insertion point, the length of the needle-electrode structure, the range of motion necessary to reach the nerve and to place the electrode within the nerve framework, a 300x400x180 mm workspace was selected for our mechanical system. Concerning the approach phase, the motion along the  $x, y$  and  $z$  axes is useful to select the insertion point on the nerve. The rotation about the  $x$  axis ( $M_x$ ) is set in a range of  $\pm 90^\circ$ .

In addition, considering the necessary space for the insertion phase we set the insertion angle in a range of  $\pm 90^\circ$  about the axis of rotation. Considering the nerve size (about 2 mm) and the length of the two kinds of needles used to pierce the nerve (16 mm for straight needle and 13 mm for  $\frac{1}{4}$  of circle needle), we set the final range of translation motion along the  $z$  axis at  $\pm 20$  mm. The same combination of a rotation and a translation are also used for the electrode placement phase.

In providing the mechanical specification of the device during the three phases, we considered the dimension of surgical area, the anatomical location of the nerve in animal

specimen, surgery accuracy. Table II summarizes the preliminary mechanical specifications for the device.

TABLE II  
MECHANICAL SPECIFICATION FOR A, I, P PHASES

Device Specifications	Value
Mx motion	$\pm 90$ (mm)
X motion	$\pm 20$ (mm)
Y motion	$\pm 20$ (mm)
Z motion	$\pm 20$ (mm)
Z precision	140 (mm)
Y precision	200 (mm)
X precision	200 (mm)

### III. INSERTION TOOL DESIGN

Figure 6 shows the first prototype version.

The device is composed by a base platform that is used as a support plane for the animal specimen. One motorized translational stage provides the positioning along y axis of the two end-effectors. An additional translation stage provides the displacement of the end effectors along the x axis. Each end effector is actuated by two motors supplying the rotation around the x axis for the approach phase; an additional motor give the same DoF for the two remaining phases.

The piercing of the nerve is provided by a combination of two motions, one along the z axis and the other about the x axis.

During the electrode placement phase, the same solution was considered. In this phase, because of the material properties [11], it is difficult to predict the exit position of the needle from the nerve. A solution formed by rubbery material, with a funnel shape, placed on the tip of the linear slide should be implemented.

#### B. Actuation

The device specifications indicated in Section II.A allowed us to select the desired actuators. In particular, a 1247-040-02 linear DC-servomotor from Faulhaber GmbH (Germany) was identified as the best available solution. This actuator provides about 140  $\mu$ m linear precision up to 40 mm of travel and thus meets our specifications.

It will be necessary to develop a needle holder by means of a hole on the base area of the linear slide, in which the needle will be lodged. Through the use of the linear actuator it is possible to achieve piercings with a linear and curvilinear paths.

With the aim of making the surgical device sensitive to the changes in force, during the second and third phases the device will be controlled in force and velocity. While during the first phase, the approach phase, the surgical robot will be controlled in position.

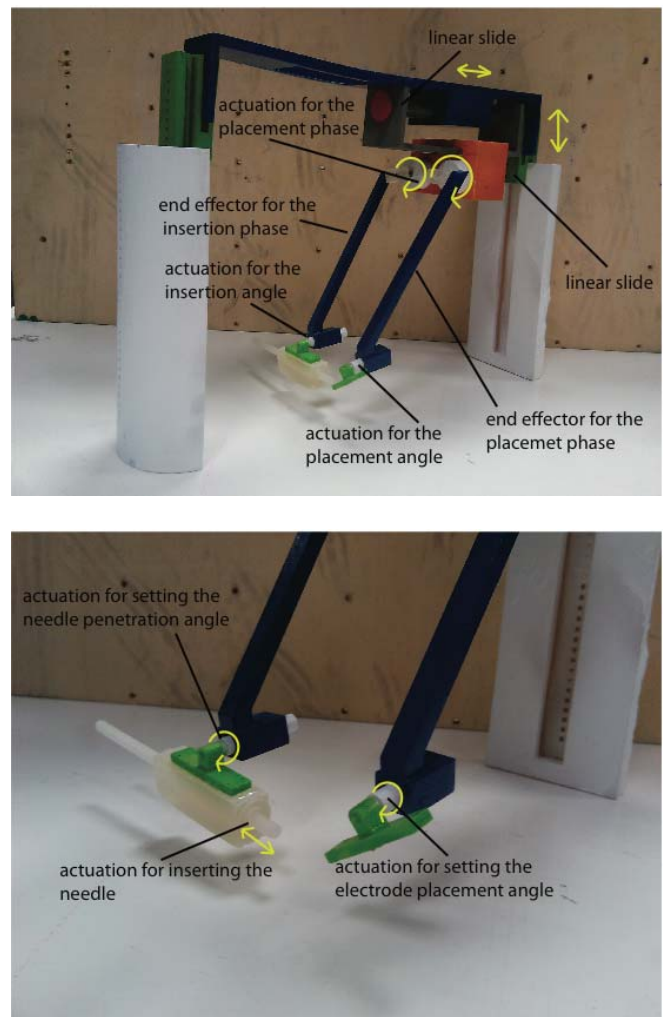


Fig. 5 Robot Mechanical System. General view (top panel) and zoomed view of the end-effector mechanism (bottom panel).

### IV. CONCLUSION AND FUTURE WORK

The paper presents a possible solution for the low accuracy and poor repeatability of hand-made intraneural electrodes. Here we focused on the development of a surgical device thought to help the surgeon during the placement of TIME electrodes into peripheral nervous tissue. We have designed and produced a first prototype of a surgical device usable for TIME electrodes insertion into the peripheral nervous system. The device can be also used as a test platform for in-vivo acquisition of force implantation data for several kinds of thin film electrodes.

Results shows that the velocity of insertion has influence in force profile and maximal force peak reached during the insertion. In particular, considering forces curves generated from higher velocity we noted that more smoothed curves can be achieved. This could suggest that at a level of velocity, in the range of cm/sec, the non-homogeneity of the tissue is not much evident. Further experiments will focus on a wider range of velocities and on the evaluation of forces involved during the electrodes placement.

## ACKNOWLEDGMENT

We thank Prof. Xavier Navarro of Universidad Autònoma de Barcelona (UAB) for valuable and useful suggestions.

## REFERENCES

- [1] T. Boretius, J. Badia, A. Pascual-Font, M. Schuettler, X. Navarro, K. Yoshida, T. Stieglitz. "A Transverse intrafascicular multichannel electrode (TIME) to interface with the peripheral nerve". *Biosensors and Bioelectronics*, vol. 26, no. 1, pp. 62-69, Sept. 2010.
- [2] R. H. Taylor and D. Stoianovici, "Medical robotics in computer-integrated surgery," *IEEE Trans. Robot. Autom.*, vol. 19, no. 5, pp. 765-781, Oct. 2003.
- [3] F. Tendick, F. Sastry, S.S. Fearing, R.S. Fearing, M. Cohn. "Applications of micromechatronics in minimally invasive surgery". *IEEE/ASME Transactions on Mechatronics*, vol. 3, no. 1, pp. 34-42, Mar. 1998.
- [4] B. Mitchell, J. Koo, M. Iordachita, P. Kazanzides, A. Kapoor, J. Handa, G. Hager, R. Taylor. "Development and application of a new Steady-Hand Manipulator for Retinal Surgery". *IEEE International Conference on Robotics and Automation*, pp. 623-629, May 2007.
- [5] N. Lago, K. Yoshida, K. P. Koch, X. Navarro. "Assessment of Biocompatibility of Chronically Implanted Polyimide and Platinum Intrafascicular Electrodes". *IEEE Transaction On Biomedical Engineering*, vol. 54, no. 2, Feb. 2007.
- [6] J. Zhang, J. T. Roland Jr., S. Manolidis, N. Simaan. "Optimal path planning for robotic insertion of steerable electrode arrays in cochlear implant surgery". *Journal of Medical Devices*, vol. 3, no. 1, March. 2007.
- [7] M. S. Fee, A. Leonardo. "Miniature motorized microdrive and commutator system for chronic neural recording in small animals". *Journal of Neuroscience Methods*, vol. 112, no. 2, pp. 83-94.
- [8] R. Grewal, Jiangming Xu, D. G. Sotereanos, S. L-Y Woo. "Biomechanical properties of peripheral nerves". *Carpal and Cubital Tunnel Surgery*, vol 12, no. 2, pp. 195-2014, May 1996.
- [9] K. Yoshida, I. Lewinsky, M. Nielsen, M. Hylleberg. "Implantation mechanics of tungsten microneedles into peripheral nerve trunks". *Med Bio Eng Computation*, vol 45, no. 4, pp. 413-420, Apr. 2007.
- [10] M. Mahvash. and P. E. Dupont. "Mechanics of Dynamic Needle Insertion into a Biological Material". *IEEE Transaction on Biomedical Engineering*, vol. 57, no. 4, pp. 934-943, Apr. 2010.
- [11] S. P. DiMaio, and S. E. Salcudean. "Needle Steering and Motion Planning in Soft Tissue". *IEEE Transaction on Biomedical Engineering*, vol. 52, no. 6, pp. 965-974. Jun. 2005.